Recent developments in the GALILÉE-1 processing code

Cédric Jouanne[1*], and *Mireille* Coste-Delclaux[1]

[1] Université Paris-Saclay, CEA, Service d'Études des Réacteurs et de Mathématiques Appliquées, 91191, Gif-sur-Yvette, France

Abstract. This paper describes the current status of GALILÉE-1 [1], the verification and processing system for evaluated data, developed at CEA. It consists of various components respectively dedicated to read/write the evaluated data independently of the format, to diagnose inconsistencies in the evaluated data and to provide continuous-energy and multigroup data as well as probability tables for particle transport and depletion codes. All these components are written in C++ language and share the same objects. In this paper, we detail the main advances made in GALILÉE-1: Unresolved Resonance Range (URR) treatment and anisotropy data production.

1 Introduction

The GALILÉE-1 system, written in C++ language, is a verification and processing system for evaluated data. It is part of a CEA global development program dedicated to the modelling of nuclear systems. Three main components along with a user-friendly and automatic chain for creating application libraries are currently under development. These components are:

- GALION (GALILÉE-1 Input Output for Nuclear data): dedicated to read evaluated data and write produced data.
- GALVANE (GALILÉE-1 Verification of the Accuracy of Nuclear Evaluations): dedicated to verify nuclear evaluations that are GALILÉE-1 input data.
- GTREND (GALILÉE-1 TReatment of Evaluated Nuclear Data): dedicated to provide continuous-energy and multigroup data as well as probability tables.

Today, the GALILÉE-1 system has the capability to create application libraries for the Monte Carlo code TRIPOLI-4 [2] with free-gas or bound nuclei. The next important issue is the production of ACE-format application libraries for the Monte-Carlo codes MCNP [3] and TRIPOLI-5. Multigroup application libraries for deterministic transport codes will be provided later.

* Corresponding author: cedric.jouanne@cea.fr

2 GALILÉE-1 System description

The GALILÉE-1 system is built upon the GBASE component that defines and implements a set of common objects, shared by all other GALILÉE-1 components. These objects are structured with a hierarchy that is very close to the GNDS [4] one and are completely independent from the input and output data formats. As shown in Figure 1, GBASE objects are:

- initialized thanks to GALION that reads the evaluation or the structure data,
- checked and possibly corrected by GALVANE,
- used by GTREND to produce processed data.

One has to note that GALVANE and GTREND only work on GBASE objects, which allows the same verification and processing stages, independently of the evaluation format. Finally, the objects storing processed data are kept in GBASE and can be written on binary or ASCII files by GALION. A more detailed description of the GALION, GALVANE and GTREND modules can be found in reference [1].

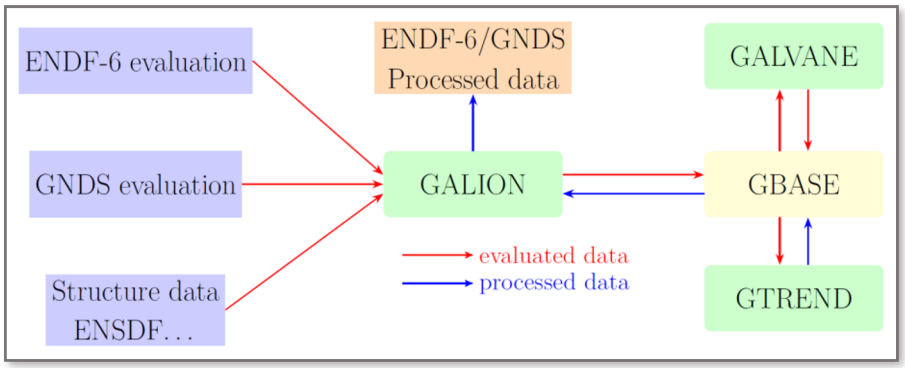

Fig. 1. GALILÉE-1 Processing Modules.

3 Probability Table calculation in the unresolved resonance range

3.1 Methodology

In order to build probability tables in the unresolved resonance range (URR), GTREND module generates random resonances by sampling resonance parameters according to the distribution laws given in the evaluations. GALILÉE-1 therefore has the capability to produce random evaluations that can be used to carry out total Monte Carlo calculations. Once these random resonance parameters are generated, GTREND has two ways of producing probability tables (PTs) in URR.

The first one (Standard PTs) is similar to the one used by CALENDF [5, 6]. URR is treated in the same manner as the resolved resonance range (RRR). Several random PENDF files, each one corresponding to one set of random resonances, are generated on the whole URR. Usually, the SLBW formalism is chosen to calculate linearized cross-sections but any other formalism could be used. Then, for each random PENDF file, cross section moments are calculated by integration methods developed in GALILÉE-1. These moments are then averaged leading to a moment-based probability table. Usually about 30 random PENDF files are used.

The second one (Monte Carlo PTs) can be used to produce either multigroup or pointwise probability tables in URR. The method consists in calculating cross-sections at various energies (either several energies in a group for multigroup PTs or given energies for pointwise PTs). It is important to notice that no linearization step (very time-consuming) is used. The sequence (generating the random resonances and calculating the cross-sections) is then repeated a large number of times in order to obtain a cross-section distribution (in each group or at each energy) that is used to calculate the moments by discrete integration. Finally, a moment-based PT is calculated. Usually, more than 50000 cross-section samples are used for a group or for a given energy.

3.2 Probability and cumulative distributions for total cross-sections

The Cs134 nucleus from the ENDF/B-VIII library is a very good candidate for comparing the NJOY/PURR [6] and GALILÉE-1/GTREND PT calculation methodologies. In that evaluation, Cs134 URR average cross-sections are calculated from the resonance parameters without adding a background cross-section. This nucleus has only two reactions in this domain: elastic scattering and radiative capture. At 5 keV (294 K), the PURR module produces a 20-step PT from 640000 cross-section calculations and the GTREND module, a 14-step PT from 100000 cross-section calculations. Figure 2 shows, on the left, the continuous cumulative distributions produced by PURR and GTREND for the total cross-section (dashed lines) as well as the discrete cumulative distributions coming from the PTs calculated by these two codes. The two continuous distributions are indistinguishable, but we observe that GTREND produces larger PT-steps values. These distribution shapes are characteristic and can be observed for all nuclei. The comparison between the continuous and the discrete cumulative distributions shows an overestimation of the discrete ones in the upper part of the high-growth area that is linked to the small point number. We can also notice that the GTREND PT models the high cross-section area more precisely than the PURR PT, despite the lower number of steps. On the right-hand side of Figure 2, the PURR and GTREND cross-sections are presented as histograms. This gives us a clearer idea of the differences between PURR and GTREND. In particular, we see an unexplained structure for the PURR distribution close to 70 barns and a different representation of the largest cross-sections.

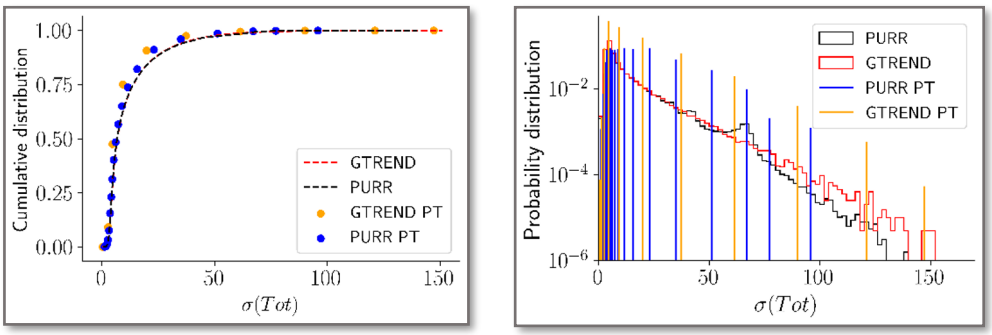

Fig. 2. Cs134 probability and cumulative distributions at 5 keV (294 K).

The structures observed on the total cross-section also exist on the elastic scattering cross-section for Cs134. Other intermediate-mass nuclei show this type of structures in the case of PURR cross-section distributions. We did not find any obvious explanation for these structures, which certainly perturb the probability tables calculated by PURR, even if this has

no significant impact on a macroscopic calculation. Figure 3 shows this type of structures for two other nuclei in the JEFF-3.3 library: Ag108 at 1 keV and Eu153 at 100 eV.

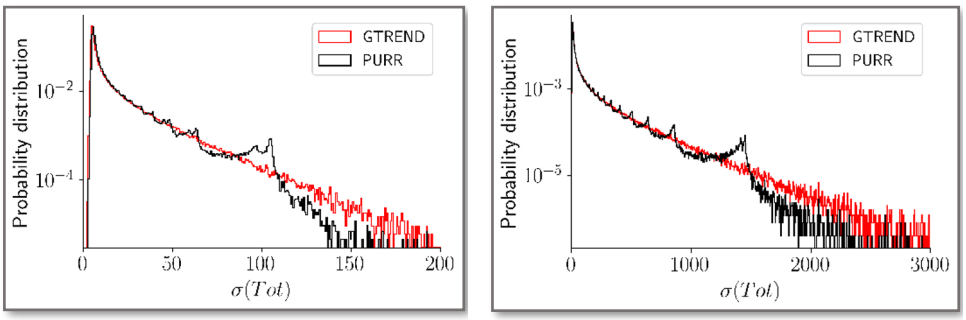

Fig. 3. Probability distributions of Ag108 at 1 keV (294 K) on the left hand side and Eu153 at 100 eV (294 K) on the right hand side.

3.3 Probability distributions for partial cross-sections

PURR and GTREND PT calculations are driven by the total cross-section, which explains the great agreement shown in Fig. 2 between the continuous and discrete cumulative or probability distributions as far as the total cross-section is concerned. That is no longer the case for a partial cross-section except when it brings the main contribution to the total cross-section.

In that section, we study the U235 nucleus coming from the ENDF/B-VIII library at 13.1 keV. For that nucleus, the contributions of the elastic scattering, radiative capture and fission cross sections are well balanced. Starting from the 640000 cross-section values calculated by PURR, we constructed the corresponding 20-step PTs with PURR and with GTREND that can handle any cross-section distribution. The PURR continuous cumulative distribution and the two PT discrete cumulative distributions are represented on Fig.4.

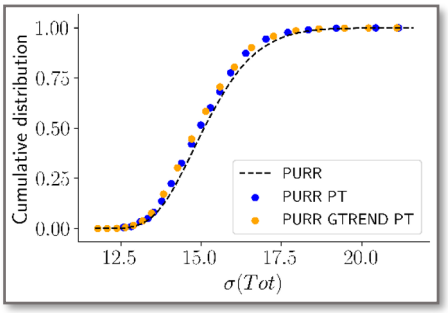

Fig. 4. Continuous and discrete cumulative distributions for U235 at 13.1 keV (294 K).

Fig. 5 shows the histograms for total cross section, elastic scattering, radiative capture and induced fission. As previously mentioned, the PT steps are defined from the total cross-section. We can see from this figure that the partial cross-sections associated with the steps do not represent the entire range of variation of each cross-sections. The lowest and highest values are quite poorly modelled by both PURR and GTREND.

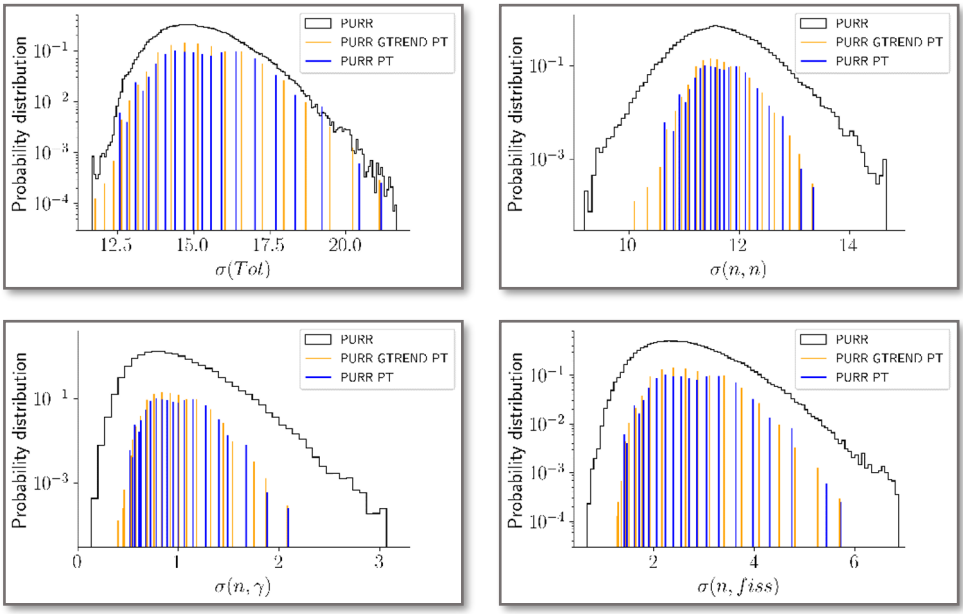

Fig. 5. Histograms and PT-step values for total and partial cross-sections of U235 at 13.1 keV (294 K).

4 Anisotropy distributions in the Resolved Resonance Range

In the case of R-Matrix Limited or Reich-Moore modelling for the resolved resonance domain, it is possible to reconstruct the anisotropies of outgoing particles. To do this, the Blatt-Biedenharn formalism is used, which produces anisotropies in the form of a series of Legendre polynomial coefficients. NJOY2016 uses the cross-section linearization grid as an energy grid for calculating angular distributions. This generates a very significant increase in the volume of reconstructed data that will be used by the Monte Carlo simulation codes. Meanwhile, GALILÉE-1 has the capability of directly linearizing the Legendre coefficients on a dedicated energy grid that can be calculated with an accuracy criterion given by the user. In this article, we focus on the anisotropy of elastic scattering.

We consider first the O16's evaluation from JEFF4T2 for which three reactions are described with the R-Matrix Limited formalism: elastic scattering, radiative capture and (n,alpha) reactions. The resolved energy range for this nucleus spans from 10^{-5} eV to 6 MeV.

Table 1 compares the number of energies for which the elastic scattering anisotropies are available in the evaluation with the number of energies produced by NJOY2016 (0.1% reconstruction criterion for cross-sections), and by GTREND (0.1%, 1% and 5% reconstruction criteria for anisotropy data). By relaxing this criterion, the GTREND grid decreases to achieve at 5%, a size close to that of the evaluation. Figure 6 shows the first-order coefficients of Legendre polynomials for the evaluation data and for the data reconstructed using NJOY and GTREND as well as the elastic scattering cross-section (left-hand scale). The evaluation's energy mesh for angular distribution does not strictly follow the cross section fluctuations and we clearly observe a lack for the first coefficient for many resonances, for example at 1.69 MeV.

Table 1. Size of energy grid for O16 (JEFF4T2) elastic angular distribution.

Anisotropy	Evaluation	NJOY2016 (0.1%)	GTREND (0.1%)	GTREND (1%)	GTREND (5%)
Energy grid	1015	4735	4409	1685	1 349

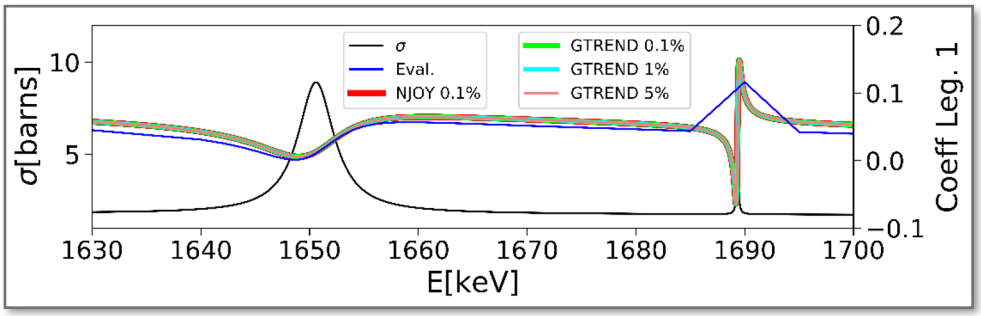

Fig. 6. O16 (JEFF4T2): Cross section and first Legendre coefficients for elastic scattering close to 1.67 MeV.

We consider then the Cl35 elastic scattering from the ENDF/B-VIII library, where the resolved range given in R-Matrix Limited formalism is from 10^{-5} eV to 1.2 MeV.
Table 2 shows the number of energies for which the anisotropies are given in the evaluation file and the number of energies calculated by NJOY or GTREND for the same reconstruction criteria as for O16. Figure 7 shows the first-order Legendre coefficient around 1.1 MeV. As for O16, the energy mesh used in the evaluation file does not allow us to follow the fluctuations linked to resonances.

Table 2. Size of energy grid for Cl35 (ENDF/B-VIII) elastic angular distribution

Anisotropy	Evaluation	NJOY2016 (0.1%)	GTREND (0.1%)	GTREND (1%)	GTREND (5%)
Energy grid	20	25788	18022	6411	3613

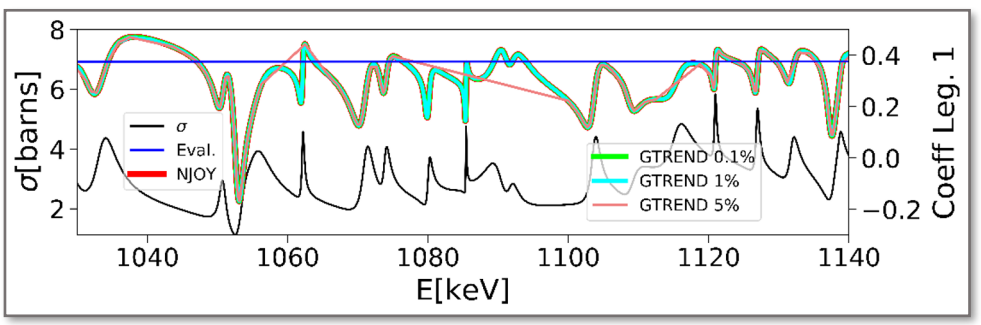

Fig. 7. Cl35 (ENDF/B-VIII): Cross section and first Legendre coefficients for elastic scattering close to 1.1 MeV.

In order to investigate the impact of these differences on the anisotropy distributions, we have calculated with the TRIPOLI-4 code a very simple slowing-down configuration in a spherical mono-atomic medium of Cl35 with a mono-kinetic punctual source (1.2 MeV) at the centre of the sphere. Figure 8 shows the resulting relative differences in neutron flux. The evaluation distribution is taken as the reference. All the calculations with the reconstructed anisotropies are in very good agreement but their discrepancies with the reference calculation can be as high as 25%. Therefore, in this particularly sensitive configuration, the impact of the reconstructed angular distributions of elastic scattering can be very significant.

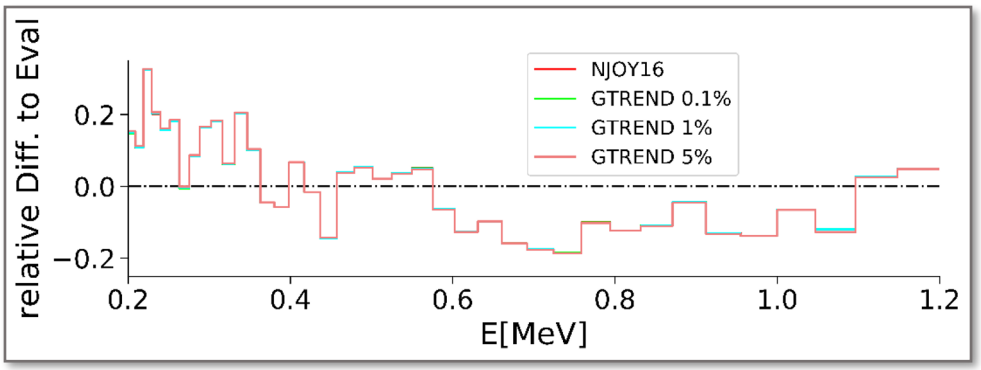

Fig. 8. Cl35 (ENDF/B-VIII): Neutron flux relative differences in slowing down calculation.

5 Conclusion

GALILÉE-1 has now the capability to prepare a complete library for TRIPOLI-4: resonances reconstruction, linearization, Doppler broadening, probability tables and thermal scattering laws processing.
In this article, we first focus on the production of probability tables in the unresolved domain. The two equivalent approaches developed by GTREND make it possible to replace the CALENDF PTs and those from the NJOY/PURR module with a good consistency. The modularity and precision of the processing give us great confidence in the results obtained.
The quality of the angular distributions of elastic and inelastic scattering is important because the energy and angular distributions of neutrons can have a major impact on neutron propagation. The R-Matrix-Limited formalism, which is increasingly used, enables the reconstruction of these distributions. In this article, we present the particular feature of GALILÉE-1 that linearizes these distributions with a user precision criterion. It clearly seems essential to reconstruct the anisotropies from the resonance parameters, given the large fluctuations of the Legendre coefficients. However, this will particularly affect the evaluations of light nuclei for neutrons of high energy.

References

1. M. Coste-Delclaux et al., EPJ Web of Conf. **239,** 10002 (2020)
2. E. Brun et al., ANE **82**, 151 (2015)
3. T. Goorley et al., Nuclear Technology **180(3)**, 298 (2012)
4. D. Brown et al., NDS **148**, 1 (2018)
5. J.C. Sublet et al., **CEA-R-6227**, (2011)
6. J.C. Sublet et al., **CEA-R-6277**, (2011)
7. R.E. MacFarlane et al., LANL, **PSR-480**, 7, (2000)